3. S.A.Sheffield, D.D.Bloomquist, C.M.Tarver, // J. Chem. Phys., 1984, 80 (8), pp. 3831-3844.
4. Е.В.Шорохов, Б.В.Литвинов, // Химическая физика, 1993, т. 12, №5, с. 722-723.
5. S.N.Lubyatinsky, B.G.Loboiko, // Detonation Reaction Zones of Solid Explosives // Proc. of 12th Symp. on Detonation.: Snowmass, Colorado, USA, 1998.
6. А.В.Фёдоров, А.Л.Михайлов, Л.Л.Антонюк, Д.В.Назаров., С.А.Финюшин // ФГВ. 2011. т. 47, №5.
7. А.В.Фёдоров // Химическая физика. 2005. т.24, №10. с. 13-21.
8. А.В.Фёдоров, А.Л.Михайлов, Л.Л.Антонюк, Д.В.Назаров., С.А.Финюшин Определение параметров зоны химической реакции, состояний пика Неймана и Чепмена-Жуге в гомогенных и гетерогенных ВВ. // Сб. тезисов XII Международной конференции Забабахинские научные чтения, 02-06 июня 2014 г.,Снежинск, с.94.
9. С.А.Колесников, А.В.Уткин, В.М.Мочалова, А.В.Анантин, // ФГВ, 2007, т.43, №6.
10. Е.А.Козлов, В.И.Таржанов, И.В.Теличко, А.В.Воробьёв, К.В.Левак, В.А.Маткин., А.В.Павленко, С.Н.Малюгина, А.В.Дулов, // Структура зоны реакции детонирующего мелкозернистого ТАТБ // Труды SWCM-2012, Киев, с. 58-60, 2012.
11. Е.А.Козлов, В.И.Таржанов, И.В.Теличко, А.В.Воробьёв, К.В.Левак, В.А.Маткин., Д.П.Кучко, М.А.Ральников, Д.С.Боярников, А.В.Павленко, С.Н.Малюгина, А.В.Дулов, // Структура зоны реакции ТАТБ при нормальной и пересжатой детонации // Международная конференция XV Харитоновские тематические научные чтения, 18 марта – 22 марта 2013 г., г. Саров.
12. R.E.Duff, E.F.Houston, // J. Chem. Phys., 1965, 23, 1268.
13. А.Н.Дремин, П.Ф.Похил, // Журнал физической химии, 1961, 34 (11), 2561.
14. Я.Б.Зельдович, А.С.Компанеец. Теория детонации.– М.: 1955, 268 с.
15. Е.А.Козлов, В.И.Таржанов, И.В.Теличко, Д.Г.Панкратов, Д.П.Кучко, М.А.Ральников, О совмещении методик оптического рычага и лазерно-гетеродинной для изучения динамических свойств конструкционных материалов // Сб. тезисов XII Международной конференции Забабахинские научные чтения, 02-06 июня 2014 г., Снежинск, с. 229
16. O.T.Strand, D.R.Goosman, C.Martinez, T.L.Whitworth, W.W.Kuhlow, // Rev. Sci. Instr., 2006, 77, 083108.
17. Ю.А.Аминов, Ю.Р.Еськов, М.М.Горшков, В.Т.Заикин, Г.В.Коваленко, Ю.Р.Никитенко, Г.Н.Рыкованов, // ФГВ, 2002, т. 38, №2, с. 121-124.
18. Экспериментальные данные по ударно-волновому сжатию и адиабатическому расширению конденсированных веществ / Под ред. Р.Ф.Трунина. Саров: РФЯЦ – ВНИИЭФ, 2006, 531 с.

THIN BARRIER METHOD USED TO STUDY KINETICS OF HE DECOMPOSITION NEAR THE DETONATION FRONT

V.I. Tarzhanov, A.V. Vorobiev, A.N. Eskov, D.P. Kuchko, M.A. Ralnikov, R.V. Komarov

RFNC VNIITF, Snezhinsk, Russia

Currently availableexperimental data on shock compressibility of nonreactive explosives are obtained in the low-pressure range, i.e. at $p \leq 16$ GPa [1-4]. However in recent years, the high time-resolution photoelectric and laser-interferometric methods gave parameters of both high and commercial explosives at the Neumann peak (chemical peak) and these parameters are interpreted as points of the Hugoniot adiabat for HE that remain unreacted shortly behind the detonation front [5-11]. Reasonable question arises as to how long this HE fails to react behind the detonation front and whether it continues to be non-reacting in case of repeated loading above the Neumann peak.

Consideration is given to the experimental thin-barrier method that makes it possible to record HE decomposition immediately behind the detonation front using laser-interferometry. The barrier method previously [12, 13] used the electro-contact recording to confirm the chemical peak by the detonation theory of Zeldovich, Neumann and Doring [14]. Laser interferometry is shown to open up new possibilities of the proposed method.

Experimental setup

In our experiments, both VISAR and PDV techniques [11, 15] recorded accelerating different-metal (Al, Cu, Ni) foils with the thickness of 0.03…0.3 mm, which are placed at the surface of the plastic-bonded TATB (PTATB) having the 1.12 porosity. These techniques also recorded detonation profiles through the LiF window having an Al 2.5-μm thick coating on the side of HE (Figure 1). Foils are placed on HE and pressed up with the ferrules workholder through the set of rings made from the same foil.

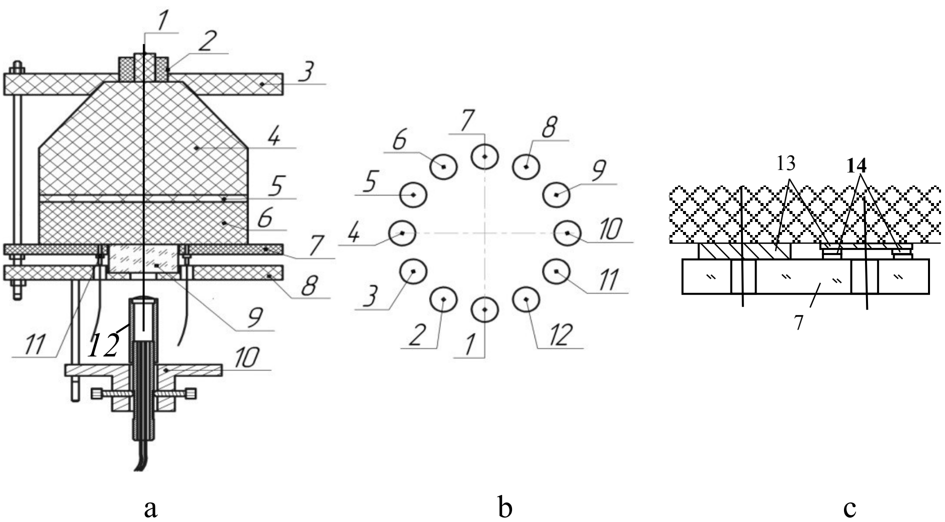

1 – electrical detonator; 2 – socket; 3 – centering mount; 4 – lens charge;
5 – TNT-RDX 50/50 cartridge with Ø120x10 mm; 6 – test HE with Ø120x40…60 mm;
7 – ferrules workholder; 8 – press-up clamp; 9 – window (LiF); 10 – measurement unit;
11 – PDV ferrules; 12 – "combined" head; 13 – foils; 14 – rings

Figure 1. Schematic experimental assembly (a), position of foils (b,c)

The initiating system comprising an electrical detonator, an explosive lens, and a TNT-RDX 50/50 cartridge served to generate the detonation wave with the plane front in the charge of the test HE. Ferrules with the 2.25-mm diameter were used to shape the probing laser beam and to receive the radiation in measurements with foils. A ferrule – is a metal cylinder with the 250-μm diameter single-mode polished-end optical fiber pasted in the axial bore thereof. Ferrules and foils were spaced 1 mm apart. Probing of the HE-LIF interface and reception of radiation therefrom in the combined head having fiber optic waveguides belonging to different techniques were performed through the use of the Ø12.7-mm optical lens with the focal distance f = 15 mm. The probing area diameter was taken to be 0.3 mm.

Results

Figrue 2 shows how initial information is processed and presented in the form of foil acceleration profiles and also shows the t, x – diagram of wave circulations in the foil. At the HE-foil interface, states with particle velocities u_1, u_2, and u_3 are observed to take place and if scattered at the foil free-surface , these states ensure velocities W_1, W_2, W_3 recorded in the form of jumps with "shelves".

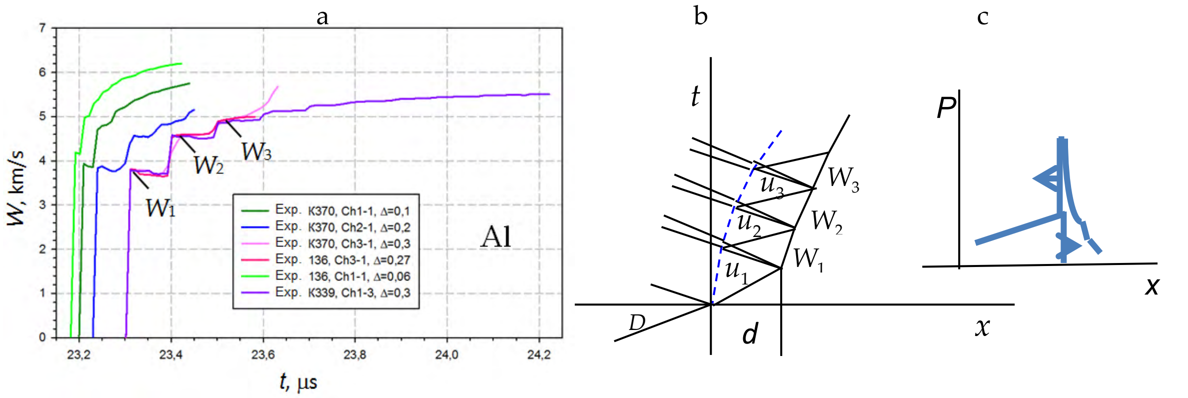

Figure 2. Acceleration profiles for different-thickness Al-foils in three experiments (a); t, x – diagram of wave circulations in the foil (b); the shaping of recompression-release profile (c)

Since the first shock wave that enters the foil is attenuating while it travels through the foil thickness, it would be incorrect to use the values W_1, W_2 and W_3 directly for determining the state in HE, which arises just after breakout of discontinuity at the “HE-foil material” interface. The particle velocities at this interface are to be calculated from the free-surface velocities W_{01}, , W_{02} and W_{03} of the zero-thickness foil. This velocity can be found by extrapolating the experimental dependencies of W_1, W_2 and W_3 on the foil thickness d till intersection with the Y-axis (Figure 3). This method is actually the virtual probing method for HE states near the detonation front within the maximally short time being close to zero.
прямое использование значений W_2 и W_3

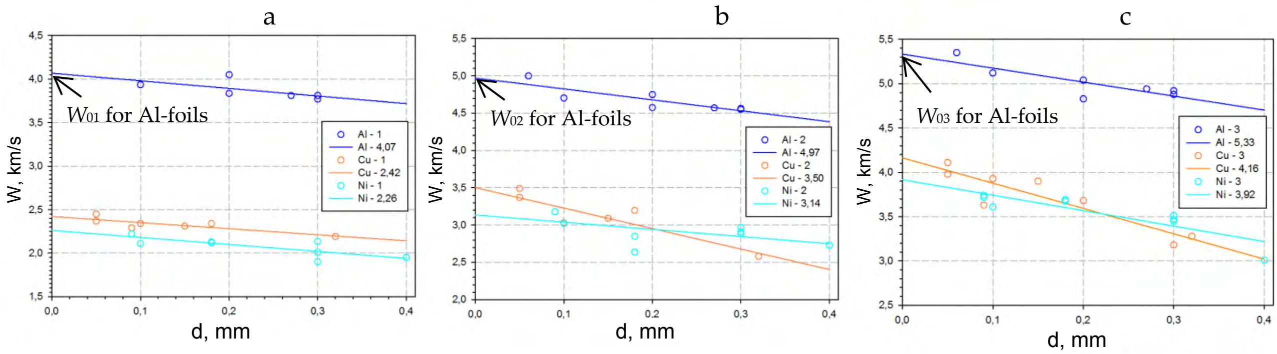

Figure 3. Recorded free-surface velocities of Al, Cu, and Ni-foils at the first jump – W_1 (a), second jump – W_2 (b), and third jump – W_3 (c) versus foils thickness. Determination of W_{01}, W_{02}, and W_{03}

Table and Figure 4 give the calculated free-surface velocities W_{01}, W_{02}, W_{03}, as well as the appropriate particle velocities u_{01}, u_{02}, u_{03} and also pressures P_{01}, P_{02}, P_{03}, which were found by the P, u – diagram methods.

Table . Calculated W_{01}, W_{02}, W_{03}, as well as appropriate particle velocities u_{01}, u_{02}, u_{03} and pressures P_{01}, P_{02}, P_{03}

Foil material	W_{01}, km/s	W_{02}, km/s	W_{03}, km/s	u_{01}, km/s	u_{02}, km/s	u_{03}, km/s	P_{01}, GPa	P_{02}, GPa	P_{03}, GPa
Al	4.07	4.97	5.33	2.035	4.52	5.15	44.7	7.41	2.73
Cu	2.42	3.50	4.16	1.21	2.96	3.83	62.1	23.0	13.0
Ni	2.26	3.14	3.92	1.13	2.70	3.53	63.2	20.2	17.4

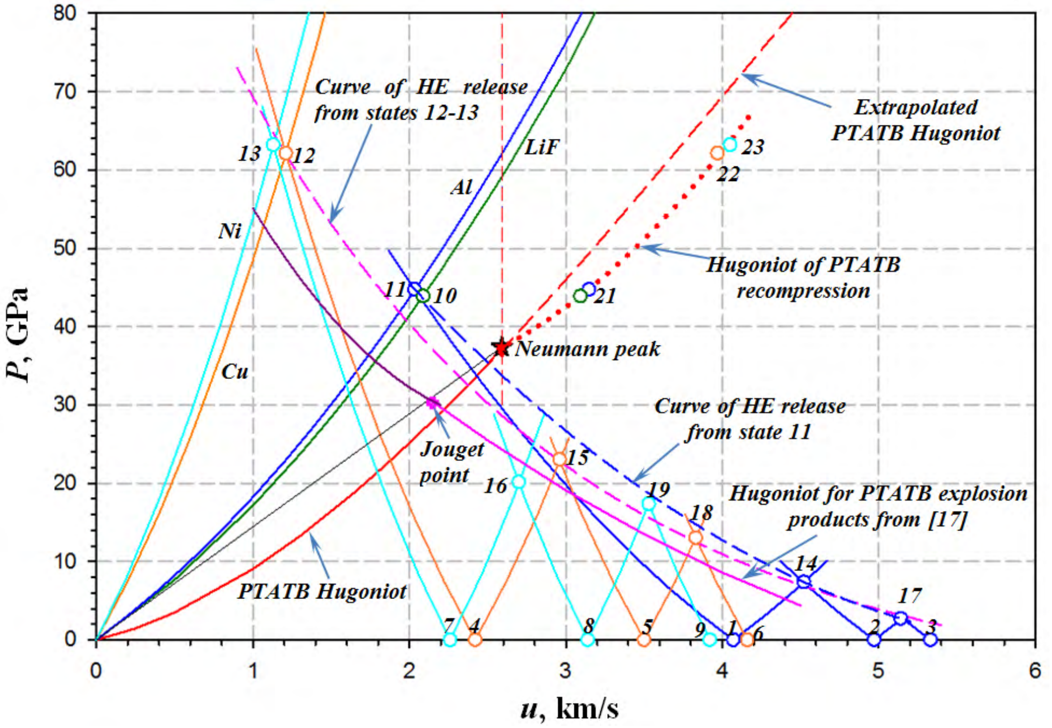

Figure 4. The P, u –diagram of states in foil materials, LiF, and test HE, observed in wave interactions

Dots (circles): 1, 2, 3 – are Al foil's free-surface velocities at the first, second, and third jumps – W_{01Al}, W_{02Al}, W_{03Al} – when foil thickness $d \to 0$; 4, 5, 6 – idem for Cu foil – W_{01Cu}, W_{02Cu}, W_{03Cu} ; 7, 8, 9 – idem for Ni foil – W_{01Ni}, W_{02Ni}, W_{03Ni} ; 10 – is particle velocity at the HE-LiF interface, 11, 12, 13 – are states on the Al, Cu, and Ni Hugoniots found from W_{01Al}, W_{02Al}, W_{03Al}, W_{01Cu}, W_{02Cu}, W_{03Cu}, W_{01Ni}, W_{02Ni}, W_{03Ni} when these states are observed as the detonation front (Neumann state) arrives at the foil; 14, 15, 16 – are states at the HE – foil material interface after the first wave circulation in the foil of aluminum, copper, and nickel; 17, 18, 19, – idem after the second wave circulation in the foil; 20 21, 22, 23, – are HE states 10 – 13 found by points when these states are observed immediately after the detonation front reflection from the foil and when they belong to the desired reloading Hugoniot;

O – state at the HE-LiF boundary in the case of detonation front arrival. This state is averaged over three experiments;

★ – state at the Neumann peak in PTATB. This state is found from **O**.

Chemical peak brake curve

Determination of states in the plastic-bonded TATB on the recompression Hugoniot is the following. First, values of W_{01} for all foil materials are used to find corresponding particle velocities in these materials with the help of the well-known relationship $u_{01} = W_{01}/2$. Then, pressures P_{01} are determined from u_{01} using interpolation equations of Hugoniots for foil materials from [18]. In Figure 4, these are states 11, 12, and 13 for Al, Cu, and Ni, respectively. It is obvious that these states simultaneously turn out to be the states of PTATB after detonation front reflection from an appropriate foil. State 10 in LiF is simultaneously the HE state after breakout of discontinuity at the HE-LiF interface. Thus, points 10, 11, 12, and 13 are observed to be the points on the Hugoniot of HE reloading from the state in the chemical peak. The Hugoniot convexity shall face left as this was HE counter loading in the case of reflection from the foil. This adiabate can be named chemical peak brake curve.

States in the plastic-bonded TATB after single and double release of foils

Values of W_{01} and W_{02} for all foil materials were used to find states 14, 15, and 16 with particle velocities u_{02} in these materials invoking the relation $u_{02} = W_{01} + (W_{02} - W_{01})/2$. Then, pressures P_{02} are determined from u_{02} using Hugoniots for foil materials. States 17, 18, and 19 (Figure 4) with particle velocities u_{03} in these materials were found from the relationship $u_{03} = W_{02} + (W_{03} - W_{02})/2$. Pressures P_{03} were calculated from u_{03} using Hugoniots of foil materials. It is obvious that both states 14 – 16 and states 17 – 19 are simultaneously states of PTATB after, respectively, single and doulbe releases from the reloading states 11 – 13. Figure 4 shows release curves that approximate the experimental data. One can see that these release curves go above the equilibrium explosion-product Hugoniot with the Jouget point from [17] thereon. It is easy to explain this location, i.e. HE was released from states 11 – 13 observed in the chemical reaction zone above the Jouget point. Note that the obtained release curves would not merge with the explosion-product Hugoniot from [17] during the follow-on wave circulations in foils as the excess energy acquired by the material in the course of reloading remains therein during release as well.

Wave profiles in the plastic-bonded TATB. Chemical peak (Neumann peak)

Figure 6 shows recorded profiles of a detonation wave in PTATB at the boundary with LiF. The mean of the maximum velocity for profiles observed in three experiments is 2.084 km/s. Pressure in LiF, which corresponds to this particle velocity, will be 43.8 GPa. This state in LiF (point 10 in Figure 4) is simultaneously the state in the PTATB, realized under its reloading on LiF from the state in the chemical peak.

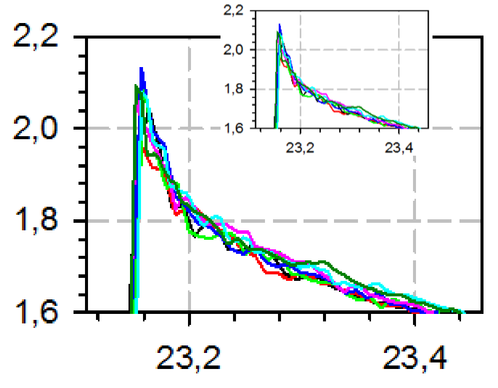

Figure 5. Seven profiles of the detonation wave in PTATB at the boundary with the LiF window. These profiles are recorded in two experiments

Discussion

The goal of this paper is to give an answer to the question dealing with physics: whether these are explosion products that accelerate foils after the detonation front arrival thereat or perhaps this is still non-reacted inert HE existing at chemical peak width. The foils are thin and the time needed for the waves to circulate once or twice in them can turn to be less than the period of the test PTATB decomposition zone. In this case, we can assume that during the first wave circulation (10 – 100 ns), HE fails to significantly decompose. And in addition, we extrapolate $W_i(d)$ to the zero thickness of foils, i.e. to extremely small times. From here it follows that HE shall remain solid both shortly behind the shock front of reloading, and also under “instantaneous” release.

Generally, new results obtained at times less than 10…300 ns demonstrate the proposed method to be promising for investigations of HE states in the chemical peak zone.

References

1. LASL Explosive Property Data / Eds. T.R. Gibbs, F. Popolato, University of California Press.: Berkeley, Los Angeles, London, 1980.
2. J.J.Dick, C.A.Forest, J.B.Ramsay, W.L.Seitz, // J. Appl. Phys., 1988, 63 (10).
3. S.A.Sheffield, D.D.Bloomquist, C.M.Tarver, // J. Chem. Phys., 1984, 80 (8), pp. 3831-3844.
4. E.V.Shorokhov, B.V.Litvinov, // J. Chem. Phys. 1993, т. 12, №5, с. 722-723.
5. S.N.Lubyatinsky, B.G.Loboiko, // Detonation Reaction Zones of Solid Explosives // Proc. of 12th Symp. on Detonation.: Snowmass, Colorado, USA, 1998.

6. A.V.Fedorov, A.L.Mikhailov, L.L.Antonyuk, D.V.Nazarov, S.A.Finyushin, // Combustion Explosion and Shock Waves (Fizika Goreniya i Vzryva), 2011, V. 47, No.5.
7. A.V.Fedorov, // J. Chem. Phys., 2005, V.24, No.10, pp.13-21.
8. A.V.Fedorov, A.L.Mikhailov, L.L.Antonyuk, D.V.Nazarov, S.A.Finyushin, Determination of Parameters of Chemical Reaction Zone and Chapman-Jouguet State in Homogeneous HE and Heterogeneous HE. // Book of Abstracts for XI International Conference "Zababakhin Scientific Talks", June 02-06, 2012, Snezhinsk, p.94.
9. S.A.Kolesnikov, A.V.Utkin, V.M.Mochalova, A.V.Anantin, // Combustion Explosion and Shock Waves (Fizika Goreniya i Vzryva). 2007. V.43, No. 6.
10. E.A.Kozlov, V.I.Tarzhanov, I.V.Telichko, A.V.Vorobiov, K.V.Levak, V.A.Matkin, A.V.Pavlenko, S.N.Malyugina, A.V.Dulov, Reaction Zone Structure for the Detonating Fine-Grained TATB // Proceedings of SWCM-2012, Kiev, pp. 58-60, 2012.
11. E.A.Kozlov, V.I.Tarzhanov, I.V.Telichko, A.V.Vorobiov, K.V.Levak, V.A.Matkin, D.P.Kuchko, M.A.Ralnikov, D.S.Boyarnikov, A.V.Pavlenko, S.N.Malyugina, A.V.Dulov, TATB Reaction Zone Structure under Normal and Overdriven Detonation // International conference "XV Khariton's Topical Scientific Readings", March 18 – 22, 2013, Sarov.
12. R.E.Duff, E.F.Houston, // J. Chem. Phys., 1965, 23, 1268.
13. A.N.Dremin, P.F.Pokhil, // J. Phys.Chem., 1961, 34 (11), 2561.
14. Ya. B.Zeldovich, A.S.Kompaneets. Detonation theory.–M.: 1955, 268 p.
15. E.A.Kozlov, V.I.Tarzhanov, I.V.Telichko, D.G.Pankratov, D.P.Kuchko, M.A.Ralnikov, On Combining the Optical Lever and Laser Heterodyne Techniques to Study Dynamic Properties of Structural Materials // Book of Abstracts for XII International Conference "Zababakhin Scientific Talks", June 02-06, 2014, Snezhinsk, p.229.
16. O.T.Strand, D.R.Goosman, C.Martinez, T.L.Whitworth, W.W.Kuhlow, // Rev. Sci. Instr., 2006, 77, 083108.
17. Yu.A.Aminov, Yu.R.Eskov, M.M.Gorshkov, V.T.Zaikin, G.V.Kovalenko, Yu.R.Nikitenko, G.N.Rykovanov, // Combustion Explosion and Shock Waves (Fizika Goreniya i Vzryva). 2002. V.38, No. pp 121-124.
18. Experimental Data on Shock-Wave Compression and Adiabatic Expansion of Condensed Materials / Edited by R.F.Trunin. Sarov: RFNC-VNIIEF, 2006, 531 p.

ЛАЗЕРНОЕ ИНИЦИИРОВАНИЕ СВЕТОЧУВСТВИТЕЛЬНОГО ВЗРЫВЧАТОГО СОСТАВА НА ОСНОВЕ ГЕКСОГЕНА ПО ПОВЕРХНОСТИ ПЛОЩАДЬЮ ~ 1000 мм²

Н.П. Хохлов, Н.А. Понькин, И.А. Лукьяненко, А.В. Руднев, О.М. Луковкин, Ю.В. Шейков, С.М. Батьянов

РФЯЦ ВНИИЭФ, Саров, Россия

Введение

В ИФВ проводятся систематические исследования воздействия лазерного излучения на светочувствительные взрывчатые составы (СВС). В результате этих исследований предложены рецептуры СВС на основе ряда высокодисперсных бризантных ВВ с добавлением нанодисперсного алюминия, а также разработаны малогабаритные светочувствительные элементы диаметром 5 мм с использованием СВС, в которых пороговая плотность энергии инициирования составляет ~ 0,5 Дж/см² [1]– [3].